ADVANCES IN ATMOSPHERIC SCIENCES, VOL. 29, NO. 3, 2012, 455–463

Sunglint Impact on Atmospheric Soundings from Hyperspectral Resolution Infrared Radiances

YAO Zhigang*(姚志刚), Jun LI, and Jinlong LI

Cooperative Institute for Meteorological Satellite Studies,

University of Wisconsin-Madison, 1225 *West Dayton Street, Madison, WI* 53706*, USA*

(Received 21 February 2011; revised 9 September 2011)

ABSTRACT

The mid-wave infrared band (3–5 μm) has been widely used for atmospheric soundings. The sunglint impact on the atmospheric parameter retrieval using this band has been neglected because the reflected radiances in this band are significantly less than those in the visible band. In this study, an investigation of sunglint impact on the atmospheric soundings was conducted with Atmospheric InfraRed Sounder observation data from 1 July to 7 July 2007 over the Atlantic Ocean. The impact of sunglint can lead to a brightness temperature increase of 1.0 K for the surface sensitive sounding channels near 4.58 μm. This contamination can indirectly cause a positive bias of 4 g kg^{-1} in the water vapor retrieval near the ocean surface, and it can be corrected by simply excluding those contaminated channels.

Key words: atmospheric sounding, hyperspectral resolution infrared radiances, sunglint

Citation: Yao, Z. G., J. Li, and J. L. Li, 2012: Sunglint impact on atmospheric soundings from hyperspectral resolution infrared radiances. *Adv. Atmos. Sci.*, **29**(3), 455–463, doi: 10.1007/s00376-011-1013-8.

1. Introduction

The sun produces very powerful radiation through the entire electromagnetic spectrum, although the radiation decreases rapidly with increasing wavelength from its spectral radiance peaks in the visible band (Závody and Birks, 2004). The contribution reflected by the sea surface is highest in the sunglint areas where the sea surface acts as a specular reflector. For the undulating oceanic surface, diffuse reflection is expected, and the reflected solar radiation is much less than the theoretical value calculated from the Fresnel equations for a plane surface. Sunglint occurs commonly and contaminates an approximately elliptical area a few hundred kilometers across the track but over thousands of square kilometers along the swath in the satellite observations.

The mid-wave infrared bands (MWIR: 3–5 μm) and long-wave infrared bands (LWIR: 7–15 μm) have been used for retrieving surface and atmospheric parameters over the ocean from satellite-based instruments, such as AIRS (Atmospheric InfraRed Sounder), IASI (Infrared Atmospheric Sounding Interferometer), and MODIS (Moderate Resolution Imaging Spectroradiometer). Some channels in these wavelengths are surface sensitive and can be contaminated by sunglint.

For remote sensing of the sea surface temperature (SST), the MWIR window channels can be significantly contaminated by sunglint (Khattak et al., 1991; Singh and Ferrier, 1997). Even for the LWIR window channels, sunglint contamination has been shown to cause an increase of a few tens of millikelvins over the open ocean. The phenomenon has gone unnoticed due to the spatial variability in surface and atmospheric conditions (Závody and Birks, 2004). This contamination on MWIR window channels is dramatically larger than that on LWIR window channels and should not be neglected, and errors as large as 15 K in the MWIR channel can be caused by sunglint (Robinson et al., 1984). To some extent, surface sensitive sounding channels in the MWIR band should also be contaminated, although they are less sensitive to the surface than the window channels.

For atmospheric soundings, the MWIR band combined with LWIR channels has been widely used (Aires et al., 2002; Seemann et al., 2003; Susskind et al., 2003;

*Corresponding author: YAO Zhigang, zyao.cimss@gmail.com

Li et al., 2007; Chahine et al., 2006). However, it is difficult to observe the sunglint signal in a radiance image of the surface sensitive sounding channels due to the significant angle dependence of the brightness temperatures (BT) resulting from the slanted path of the observations and the relatively weak sensitivity of these channels to the surface reflection. As a result, the sunglint impact on atmospheric parameter retrieval from the MWIR band has not been discussed in the previous studies.

To examine the impact of sunglint on atmospheric soundings from satellites, the AIRS data over the ocean in the daytime was used in this study to retrieve atmospheric temperature and water vapor profiles with a one-dimensional variational (1DVAR) physical retrieval algorithm.

2. Data

Satellite-based hyperspectral (or advanced) infrared (IR) sounding measurements are a principal source of water vapor and temperature data over areas where conventional in situ observations are relatively sparse. Hyperspectral IR sounders such as the Atmospheric InfraRed Sounder (AIRS) onboard NASA's EOS Aqua platform, and the Infrared Atmospheric Sounding Interferometer (IASI) onboard the Europe's Metop-A satellite are providing unprecedented global atmospheric temperature and moisture profiles with high vertical resolution and accuracy. Along with an Advanced Microwave Sounding Unit (AMSU) that provides atmospheric profiles in most cloudy regions, the advanced IR sounders are able to provide soundings with much better vertical resolution, greater accuracy (e.g., 1 K for temperature, 15% for water-vapor mixing ratio) (Tobin et al., 2006), and higher spatial resolution (i.e., 12–14 km at nadir) than previous sounders. The advanced IR sounding data have been shown to be significant to atmospheric research and the monitoring of the Earth's environment (Chahine et al., 2006) as well as global numerical weather prediction (NWP) models (Le Marshall et al., 2006) and regional tropical cyclone forecast models (Li and Liu, 2009; Liu and Li, 2010).

AIRS was launched on 4 May 2002 and is the first of a new generation of high spectral resolution IR sounders. It has 2378 channels covering 649–1136 cm^{-1}, 1217–1613 cm^{-1}, and 2181–2665 cm^{-1} (8.8–15.4 μm, 6.2–8.2 μm, and 3.75–4.58 μm, respectively). AIRS is able to sense the atmospheric temperature, water vapor, trace gases, and surface skin temperature with high vertical resolution and accuracy. This instrument sweeps along its orbit gathering data that is sectioned into pieces. Each piece is called a "granule." The spatial coverage of each AIRS data granule is roughly 2250 km × 1650 km. Each cross-track swath consists of 90 fields of view (FOVs), with 13.5 km spatial resolution at nadir.

3. Method

The CIMSS (Cooperative Institute of Meteorological Satellite Studies) Hyperspectral IR Sounder Retrieval (CHISR) algorithm has been developed to retrieve atmospheric temperature and moisture profiles from advanced IR sounder radiance measurements in clear skies and some cloudy sky conditions on a single field-of-view (SFOV) basis (Li and Huang, 1999; Li et al., 2000; Wu et al., 2006; Weisz et al., 2007). In the physical retrieval, a forward model $\boldsymbol{F}(\boldsymbol{x})$ relates the state vector $\boldsymbol{x}$ to the measurements vector $\boldsymbol{Y}$. Therefore, $\boldsymbol{F}$ has the same dimension as $\boldsymbol{Y}$. Given the atmospheric parameter profiles, surface temperature, and surface emissivity, the AIRS observation vector has the form

$$\boldsymbol{Y} = \boldsymbol{F}(\boldsymbol{x}), \tag{1}$$

where the individual elements are calculated by the AIRS clear-sky fast radiative transfer model developed by Strow et al. (2003). A general form of the solution minimizes the following penalty function (Rodgers, 1976):

$$\boldsymbol{J}(\hat{\boldsymbol{x}}) = (\hat{\boldsymbol{x}} - \boldsymbol{x}_\mathrm{a})^\mathrm{T} \boldsymbol{S}_\mathrm{a}^{-1} (\hat{\boldsymbol{x}} - \boldsymbol{x}_\mathrm{a}) + [\boldsymbol{Y} - \boldsymbol{F}(\hat{\boldsymbol{x}})]^\mathrm{T} \boldsymbol{S}_\varepsilon^{-1} [\boldsymbol{Y}_\mathrm{m} - \boldsymbol{F}(\hat{\boldsymbol{x}})] , \tag{2}$$

where $\boldsymbol{x}_\mathrm{a}$ is the background information matrix of $\boldsymbol{x}$, $\boldsymbol{S}_\mathrm{a}$ is the assumed background error covariance matrix that constrains the solution, $\boldsymbol{Y}_\mathrm{m}$ is the AIRS measurements vector, and $\boldsymbol{S}_\varepsilon$ is the observation error covariance matrix, which includes instrument noise plus the assumed forward model error. To solve the equation, a Newtonian iteration is used:

$$\hat{\boldsymbol{x}}_{\mathrm{n}+1} = \hat{\boldsymbol{x}}_\mathrm{n} + \boldsymbol{J}''(\hat{\boldsymbol{x}}_\mathrm{n})^{-1} \cdot \boldsymbol{J}'(\hat{\boldsymbol{x}}_\mathrm{n}) , \tag{3}$$

and the following quasi-nonlinear iterative form (Eyre, 1989) is obtained:

$$\delta\hat{\boldsymbol{x}}_{\mathrm{n}+1} = (\boldsymbol{K}_\mathrm{n}^\mathrm{T} \boldsymbol{S}_\varepsilon^{-1} \cdot \boldsymbol{K}_\mathrm{n} + \boldsymbol{S}_\mathrm{a}^\mathrm{T})^{-1} \cdot \boldsymbol{K}_\mathrm{n}^\mathrm{T} \boldsymbol{S}_\varepsilon^{-1} \cdot (\delta\boldsymbol{Y}_\mathrm{n} + \boldsymbol{K}_\mathrm{n} \cdot \delta\hat{\boldsymbol{x}}_\mathrm{n}) , \tag{4}$$

where $\delta\hat{\boldsymbol{x}}_\mathrm{n} = \hat{\boldsymbol{x}}_\mathrm{n} - \boldsymbol{x}_\mathrm{a}$, $\delta\boldsymbol{Y}_\mathrm{n} = \boldsymbol{Y}_\mathrm{m} - \boldsymbol{Y}(\hat{\boldsymbol{x}}_\mathrm{n})$, and $\boldsymbol{K} = \partial\boldsymbol{F}/\partial\hat{\boldsymbol{x}}$ represents the linear or tangent model of the forward model $\boldsymbol{F}$, which is used to calculate the AIRS observations from the inputs, including the atmospheric parameter profiles and surface parameters. Due to a large number of unknowns in the inverse problem and the instability of the solution, it is usually difficult to retrieve the surface temperature and

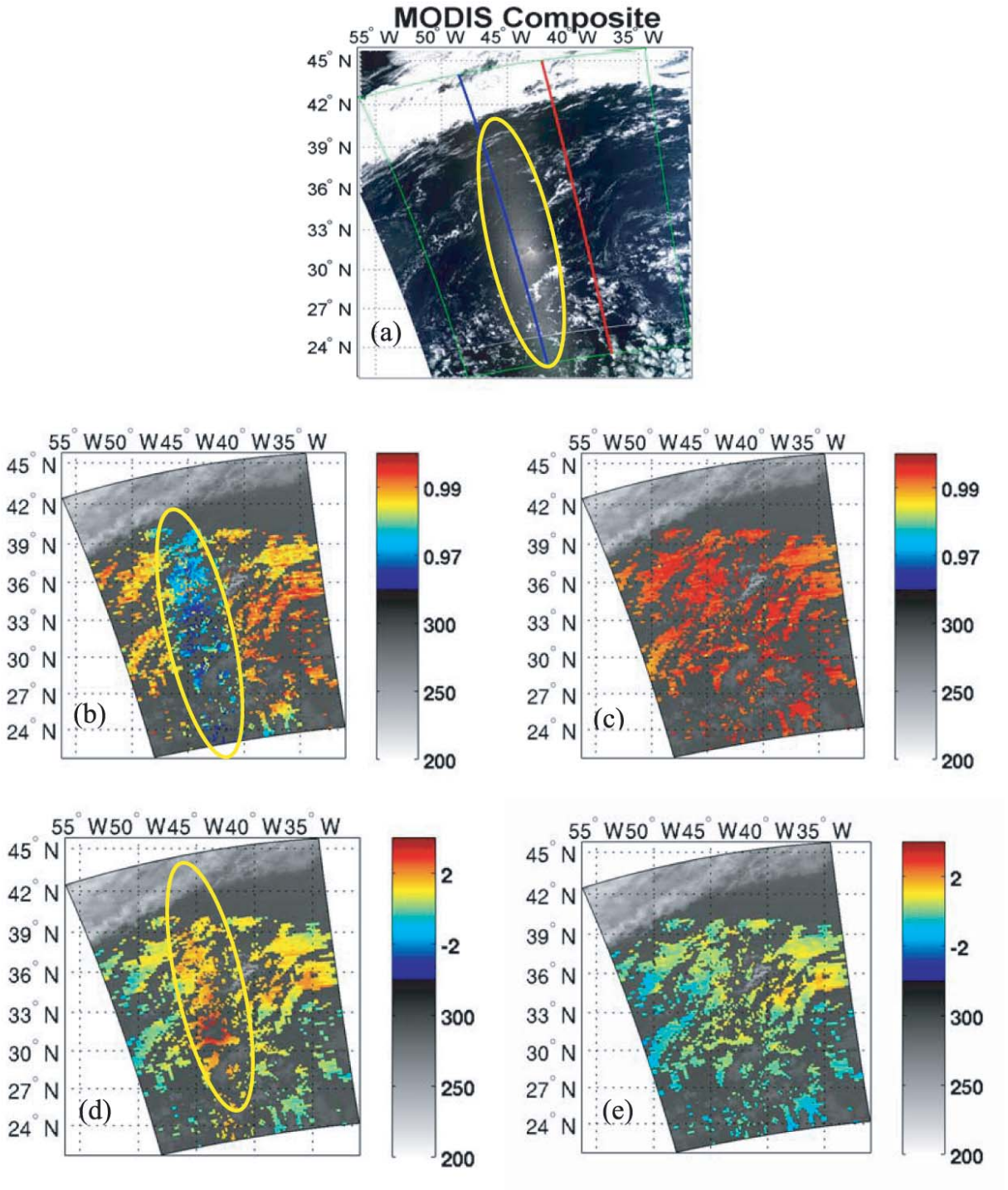

Fig. 1. (a) MODIS visible composite at 1600 UTC on 2 July 2007 (Red = 0.650 μm , Green = 0.56 μm, and Blue= 0.44 μm; the blue and red lines correspond to AIRS observation angles at -19.2° and $+19.2^\circ$, respectively; the green box represents the AIRS granule); retrieved SSE from the experiment (b) with and (c) without the MWIR channels; SST retrieval error (d) with and (e) without the MWIR channels by comparison with the ECMWF reanalysis for Granule 160 at 1600 UTC on 2 July 2007 overlaying the 11-μm brightness temperatures (K) (black/white) image. The impacted areas are denoted by yellow circles.

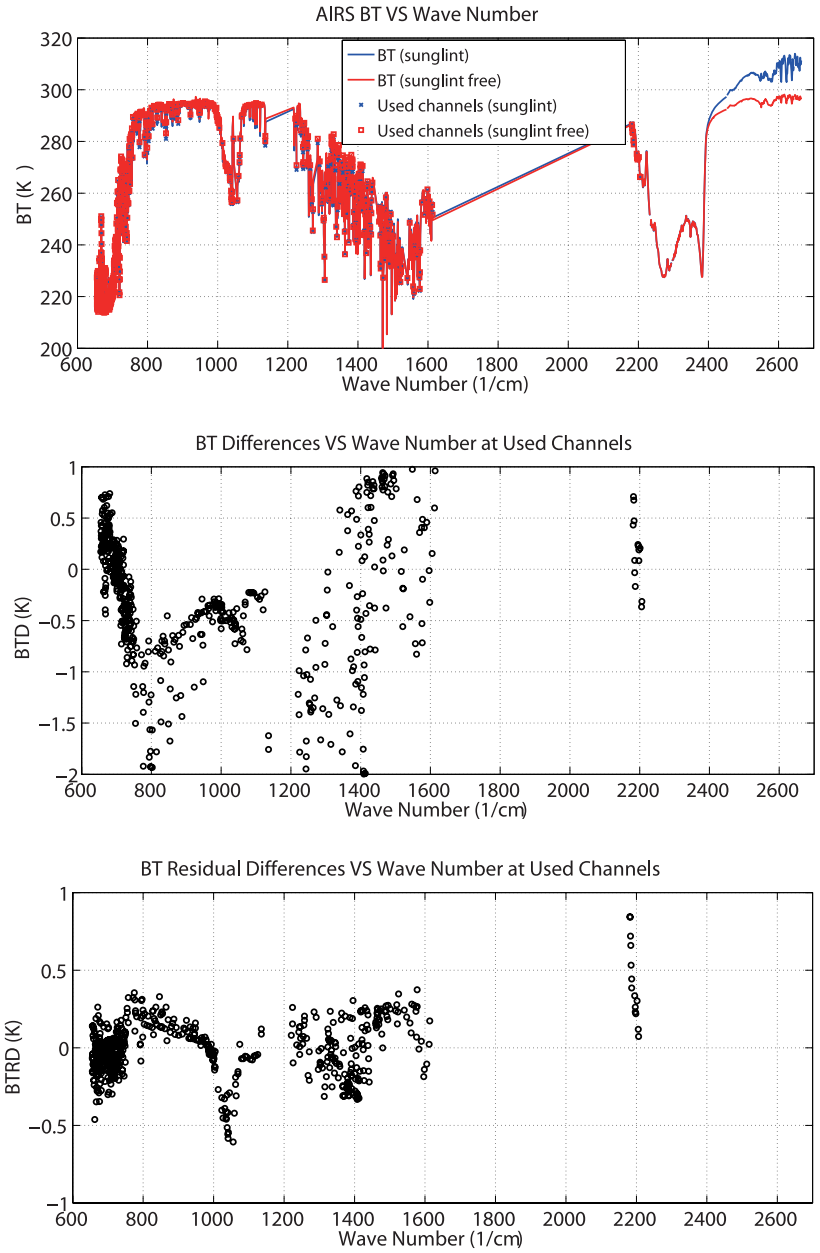

Fig. 2. (top) The mean BT spectrum in the sunglint area (angle = −19.2°) and the sunglint-free area (angle = +19.2°); (middle) the mean BT difference spectrum between the two selected observation angles; (bottom) the difference spectrum between the mean BT residuals along the two selected observation angles.

emissivity spectrum as well as atmospheric parameters directly from hyperspectral resolution IR radiances. In the CHISR algorithm, the emissivity eigenvectors (EVs) are used to represent a hyperspectral IR emissivity spectrum, so that the surface emissivity spectrum and the atmospheric parameters can be derived simultaneously from hyperspectral IR radiances in a physical iterative approach (Li et al., 2007; Li and Li, 2008). In this study, this algorithm was used to investigate the effects of the sunglint on AIRS sounding retrieval.

4. Experiments and results

In this study, an investigation of angle dependence of the retrieval, which is related to the sunglint ar-

eas, was performed for AIRS observations with the latitudes of 0°–40°N and the longitudes of 60°–30°W from 1 July to 7 July 2007 over the Atlantic Ocean. That location is one of the clearest areas affected by sunglint and allowed us to find enough cloud-free pixels at each angle. Due to the fact that the AIRS FOV is quite large (12–14 km), cloud contamination is not a negligible issue (Wei et al., 2004). Consequently, the MODIS cloud mask was used to determine the clear AIRS FOVs (Li et al., 2004). Roughly 250 samples were available at each angle. The atmospheric temperature and moisture retrieval were evaluated against the European Center for Medium-Range Weather Forecasts (ECMWF) temperature and moisture reanalysis profiles from the nearest grid point in space, which were temporally interpolated to the AIRS observation time. As a result, the retrieval comparison was easily performed with a large variety of atmospheric conditions.

To investigate the impact of sunglint in the MWIR band on the soundings from AIRS, experiments with and without this band were performed. 575 channels, including 14 MWIR channels, were used in the original algorithm. In the experiment with the MWIR observations, the sea surface emissivity (SSE) model developed by Nalli et al. (2008) was used to produce the SSE spectrum. This model was developed for remote sensing applications over ocean, which depends on sea surface wind speeds and observation angles. The emissivity look-up table is based on the Hale-Querry refractive indices and Cox-Munk wave slopes. The wind speed was set to 5 m s^{-1} because the calculation shows that the wind dependence of the emissivity is relatively weak.

For Granule 160 on 2 July 2007, the retrieved SSE at 11 μm and the SST errors from the two experiments are shown in Fig. 1. The corresponding MODIS visible composite is also shown in this figure. It can be seen that the overestimation of the SST as well as the underestimation of the SSE in the experiment with the MWIR channels correspond to the sunglint areas shown in Fig. 1a. Additionally, these biases have not been found for the AIRS granules in the night time or in sunglint-free areas. This indicates that the biases of the retrieved surface parameters are related to sunglint. Also, excluding the MWIR channels could reduce these biases. The comparison of the results from the two experiments confirms that sunglint contamination on the MWIR channels should have a great impact on surface parameter retrieval.

To quantitatively investigate the observation bias caused by sunglint, the mean BT spectrums for all channels used in the retrieval at the two symmetric observation angles represented by blue and red lines in Fig. 1a, which correspond to the sunglint areas, the sunglint-free areas, and their differences are presented in Fig. 2. In the top panel, the two BT spectra agree well because they have the same slanted observation paths when the wave number is <2400 cm^{-1}. Dramatic differences are caused by the sunglint in the channels with larger wave numbers. It appears that the sunglint has no impact on the channels used in the retrieval. However, there are noticeable differences shown in the middle panel at these selected channels. Without considering the sunglint, the differences would be attributed to the varying surface and atmospheric conditions as well as the observations uncertainties. To extract the sunglint impact on the observations, the BT residuals (observed−calculated) are derived using the ECMWF reanalysis, which can help reduce the impact of the atmosphere variation on the differences. The differences between the BT residuals along the blue and red lines are shown in the bottom panel. It can be seen that the residual differences at most of surface sensitive channels from 800 to 1000 cm^{-1} are <0.2 K, which is comparable with the observation uncertainties. However, it is clear that the BT residual differences at surface sensitive sounding channels near 2200 cm^{-1}, which are mostly affected by the sunglint in the previous selected channels, are significantly greater than those at the surface sensitive channels in the LWIR band. For this granule, the BT residuals at 4.85 μm (2182 cm^{-1}) are shown in Fig. 3. This impact could exceed 1 K in the sunglint areas. The results indicate that the sunglint has dramatic impacts on the observations at the MWIR sounding channels.

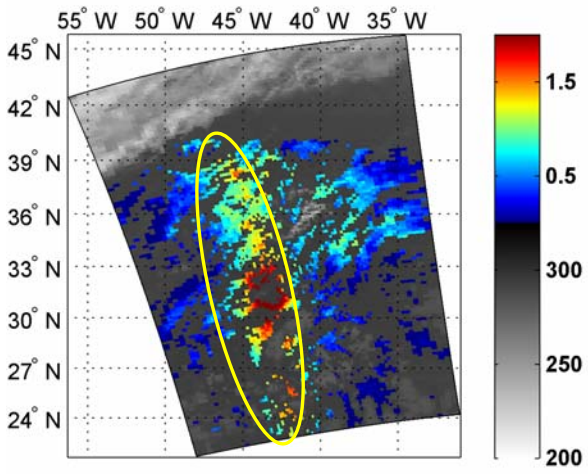

Fig. 3. The BT residuals at 4.85 μm for Granule 160 at 1600 UTC on 2 July 2007 overlaying the 11-μm brightness temperatures (K) (black/white) image. The impacted area is denoted by a yellow circle.

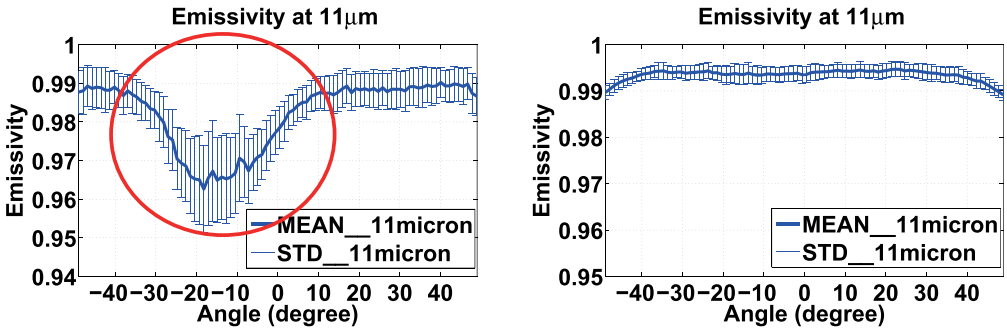

(a) Retrieved emissivity versus observation angle

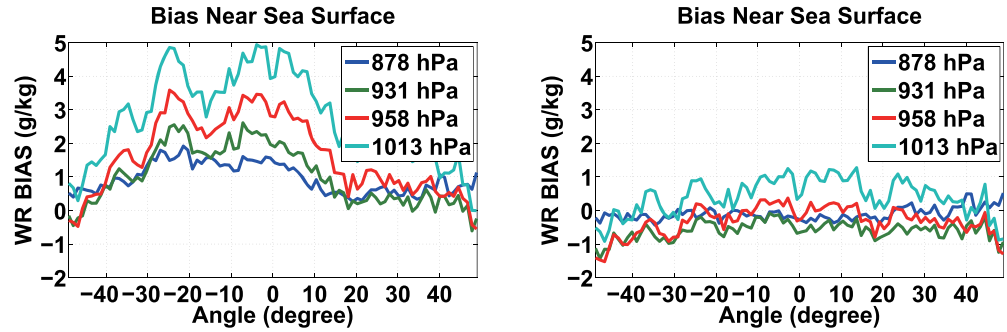

(b) Bias of the retrieved WR near surface versus observation angle

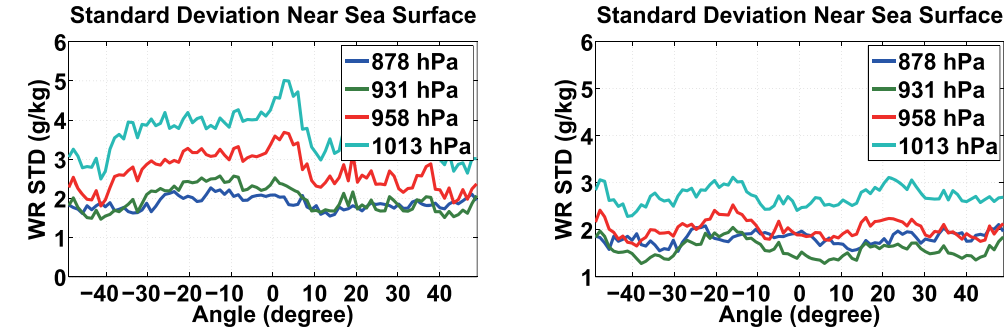

(c) Standard deviation of the retrieved WR errors near surface versus observation angle

Fig. 4. Retrieved sea surface emissivity (impacted area denoted by a red circle) and water vapor mixing ratio retrieval error at each angle from the retrieval experiments with (the left) and without (the right) the MWIR channels for the AIRS data from 1 to 7 July 2007 over Atlantic Ocean in the day time.

Actually, the water vapor mixing ratio (WR) retrieval is not directly affected by the sunglint because the MWIR channels used are mostly sensitive to surface and atmospheric temperatures near surface. As a result, the surface temperature and emissivity spectrum are impacted in the simultaneous retrieval, as shown in Fig. 1. At the same time, the errors in the retrieved surface parameters dramatically decrease the WR retrieval accuracy and precision.

To further analyze the sunglint impact on atmospheric and surface parameter retrievals, the means and standard deviations of the retrieved SSE at each angle for all clear pixels from 1 to 7 July 2007 in the selected domain were calculated and are shown in Fig. 4. The means and standard deviations of the differences between the retrieved and ECMWF reanalysis WR at four different levels near sea surface are also shown in the figure. It can be seen that the bias could exceed

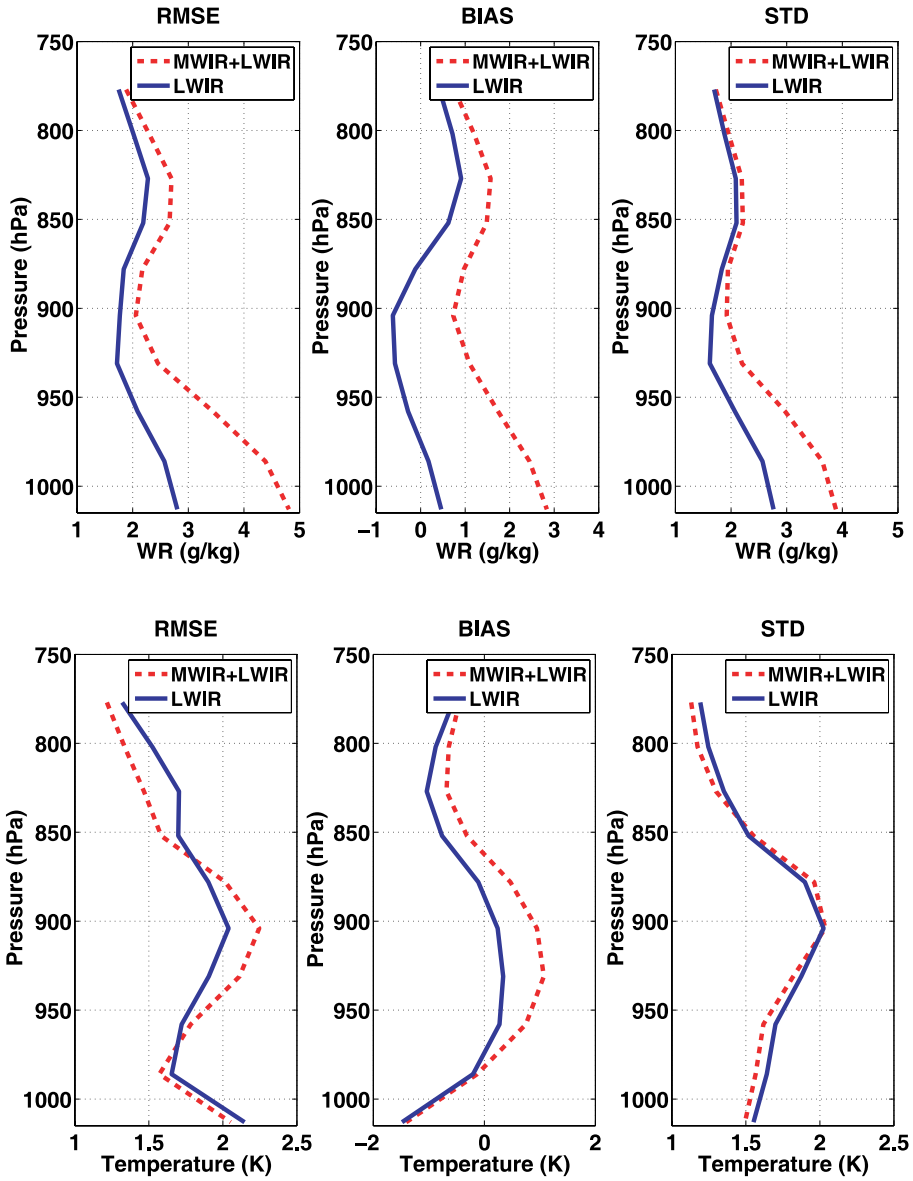

Fig. 5. (top) Water vapor mixing ratio and (bottom) temperature error statistics (RMSE: root means square error; BIAS: bias; STD: standard deviation) with and without the MWIR channels for the AIRS data (24962 clear pixels) over Atlantic Ocean from 1 July to 7 July 2007 in the day time by comparison with the ECMWF reanalysis.

4 g kg^{-1} at the level closest to the sea surface. Additionally, it is noted that this impact decreases with decreasing pressure. It may be explained by the fact that the peaks of the sounding channel weighting functions closer to the surface are more sensitive to the surface conditions. The accuracy and precision of the WR retrieval near the surface can be dramatically improved by excluding MWIR channels.

The error statistics analysis for the two experiments at all observation angles are shown in Fig. 5. The experiment without the MWIR channels obtained significantly better results than that with the MWIR radiances for the WR retrieval. Additionally, the biases in the retrieved temperature profiles from 870 to 980 hPa were reduced by excluding the MWIR channels, whereas they increased at other levels. It seems that the channels with a smaller sunglint signal should not be removed from the retrieval. However, these results suggest that these channels should be excluded to prevent possible negative impacts on the atmospheric parameter retrieval until a correction method is developed to reduce the contamination in the MWIR ob-

servations. For example, a radiative transfer model taking sunglint into account could be used to calculate the solar radiation, which would allow all possible channels in the retrieval process.

5. Summary

The sunglint impact on atmospheric parameter retrieval using surface sensitive MWIR sounding channels over the ocean has been widely neglected in the satellite data application communities. It has been indicated that sunglint leads to a BT increase of 1.0 K for some surface sensitive channels near 4.58 μm. Our comparison shows that sunglint has dramatic impacts on the WR retrieval at the pressure levels >750 hPa using AIRS MWIR radiances. Significant WR retrieval improvement can be obtained by simply excluding MWIR channels. This result can be broadly used to improve the WR retrieval accuracy over the ocean using different infrared instruments. Additionally, a sunglint correction method based on a physical model should be developed for including the contaminated sounding channels in the retrieval.

Acknowledgements. This work was partly supported by the National Oceanic and Atmospheric Administration (NOAA) GOES-R algorithm working group (AWG) and GOES-R Risk Reduction programs (Grant No. NA06NES4400002). The authors would like to specifically thank the AIRS science team for providing AIRS data and ECMWF for sharing the model output data. The authors also thank the University of Maryland–Baltimore County for providing the fast radiative transfer model (SARTA) for the sounding retrieval experiments.

REFERENCES

Aires, F., W. B. Rossow, N. A. Scott, and A. Chédin, 2002: Remote sensing from the infrared atmospheric sounding interferometer instrument 2. Simultaneous retrieval of temperature, water vapor and ozone atmospheric profiles. *J. Geophys. Res.*, **107**, D22, 4620–4631.

Chahine, M. T., and Coauthors, 2006: AIRS: Improving weather forecasting and providing new data on greenhouse gases. *Bull. Amer. Meteor. Soc.*, **87**, 911–926.

Eyre, J. R., 1989: Inversion of cloudy satellite sounding radiances by nonlinear optimal estimation I: Theory and simulation. *Quart. J. Roy. Meteor. Soc.*, **115**, 1001–1026.

Khattak, S., R. A. Vaughan , and A. P. Cracknell, 1991: Sunglint and its observation in AVHRR data. *Remote Sensing of Environment*, **37**, 101–116.

Le Marshall, J., and Coauthors, 2006: Improving global analysis and forecasting with AIRS. *Bull. Amer. Meteor. Soc.*, **87**, 891–894.

Li, J., and H.-L. Huang, 1999: Retrieval of atmospheric profiles from satellite sounder measurements by use of the discrepancy principle. *Appl. Optics*, **38**, 916–923.

Li, J., and J. Li, 2008: Derivation of global hyperspectral resolution surface emissivity spectra from advanced infrared sounder radiance measurements. *Geophys. Res. Lett.*, **35**, L15807, doi: 10.1029/2008GL034559.

Li, J., and H. Liu, 2009: Improved hurricane track and intensity forecast using single field-of-view advanced IR sounding measurements. *Geophys. Res. Lett.*, **36**, L11813, doi: 10.1029/2009GL038285.

Li, J., W. Wolf, W. P. Menzel, W. Zhang, H.-L. Huang, and T. H. Achtor, 2000: Global soundings of the atmosphere from ATOVS measurements: The algorithm and validation. *J. Appl. Meteor.*, **39**, 1248–1268.

Li, J., W. P. Menzel, F. Sun, T. J. Schmit, and J. Gurka, 2004: AIRS subpixel cloud characterization using MODIS cloud products. *J. Appl. Meteor.*, **43**, 1083–1094.

Li, J., J. Li, E. Weisz, and D. K. Zhou, 2007: Physical retrieval of surface emissivity spectrum from hyperspectral infrared radiances. *Geophys. Res. Lett.,* **34**, L16812, doi: 10.1029/2007GL030543.

Liu, H., and J. Li, 2010: An improvement in forecasting rapid intensification of Typhoon Sinlaku (2008) using clear-sky full spatial resolution advanced IR soundings. *J. Appl. Meteor. Climatol.*, **49**, 821–827

Nalli, N. R., P. J. Minnett, and P. van Delst, 2008: Emissivity and reflection model for calculating unpolarized isotropic water surface-leaving radiance in the infrared. 1: Theoretical development and calculations. *Appl. Opt.,* **47**, 3701–3721.

Robinson, I. S., N. C. Wells, and H. Charnock , 1984: The sea surface thermal boundary layer and its relevance to the measurement of sea surface temperature by airborne and spaceborne radiometer. *Int. J. Remote Sens.* **5**, 19–45.

Rodgers, C. D., 1976: Retrieval of atmospheric temperature and composition from remote measurements of thermal radiation. *Rev. Geophys.*, **14**, 609–624.

Seemann, S., J. Li, W. P. Menzel, and L. E. Gumley, 2003: Operational retrieval of atmospheric temperature, moisture, and ozone from MODIS infrared radiances. *J. Appl. Meteor.,* **42**, 1072–1091.

Singh, S. M., and G. Ferrier, 1997: Observation of intense sun glint in 3.7 μm channel of the AVHRR. *Int. J. Remote Sens.*, **18**, 3521–3533.

Strow, L. L., S. E. Hannon, S. Souza-Machado, H. E. Motteler, and D. Tobin, 2003: An overview of the AIRS radiative transfer model. *IEEE Trans. Geosci. Remote Sensing*, **41**, 303–313.

Susskind, J., C. D. Barnet, and J. M. Blaisdell, 2003: Retrieval of atmospheric and surface parameters from AIRS/AMSU/HSB data in the presence of clouds. *IEEE Trans. Geosci. Remote Sens.*, **41**, 390–409.

Tobin, D. C., and Coauthors, 2006: Atmospheric radiation measurement site atmospheric state best es-

timates for atmospheric infrared sounder temperature and water vapor retrieval validation. *J. Geophys. Res.*, **111**, D09S14, doi: 0.1029/2005JD006103.

Wei, H., P. Yang, J. Li, B. A. Baum, H.-L. Huang, S. Platnick, Y. Hu, and L. Strow, 2004: Retrieval of semitransparent ice cloud optical thickness from Atmospheric Infrared Sounder (AIRS) measurements. *IEEE Trans. Geosci. Remote Sensing*, **42**, 2254–2267.

Weisz, E., J. Li, J. L. Li, D. K. Zhou, H.-L. Huang, M. D. Goldberg, and P. Yang, 2007: Cloudy sounding and cloud-top height retrieval from AIRS alone single field-of-view radiance measurements. *Geophys. Res. Lett.*, **34**, L12802, doi: 10.1029/2007GL030219.

Wu, X. B., J. Li, W. J. Zhang, and F. Wang, 2006: Atmospheric profile retrieval with AIRS data and validation at the ARM CART site. *Adv Atmos. Sci.*, **22**(5), 647–654.

Závody, A. M., and A. R. Birks, 2004: Sun glint contamination in ATSR-2 data: Comparison of observations and values calculated from the measured 1.6-m reflectivities. *J. Atmos. Oceanic Technol.*, **21**, 787–798.